JACS
JOURNAL OF THE AMERICAN CHEMICAL SOCIETY

pubs.acs.org/JACS Article

Diastereoselective Radical Aminoacylation of Olefins through N-Heterocyclic Carbene Catalysis

Wen-Deng Liu,§ Woojin Lee,§ Hanyu Shu, Chuyu Xiao, Huiwei Xu, Xiangyang Chen, Kendall N. Houk,* and Jiannan Zhao*

Cite This: *J. Am. Chem. Soc.* 2022, 144, 22767−22777 Read Online

ACCESS | Metrics & More | Article Recommendations | Supporting Information

ABSTRACT: There have been significant advancements in radical-mediated reactions through covalent-based organocatalysis. Here, we present the generation of iminyl and amidyl radicals via N-heterocyclic carbene (NHC) catalysis, enabling diastereoselective aminoacylation of trisubstituted alkenes. Different from photoredox catalysis, single electron transfer from the deprotonated Breslow intermediate to *O*-aryl hydroxylamine generates an NHC-bound ketyl radical, which undergoes diastereocontrolled cross-coupling with the prochiral C-centered radical. This operationally simple method provides a straightforward access to a variety of pyrroline and oxazolidinone heterocycles with vicinal stereocenters (77 examples, up to >19:1 d.r.). Electrochemical studies of the acyl thiazolium salts support our reaction design and highlight the reducing ability of Breslow-type derivatives. A detailed computational analysis of this organocatalytic system suggests that radical−radical coupling is the rate-determining step, in which $\pi-\pi$ stacking interaction between the radical intermediates subtly controls the diastereoselectivity.

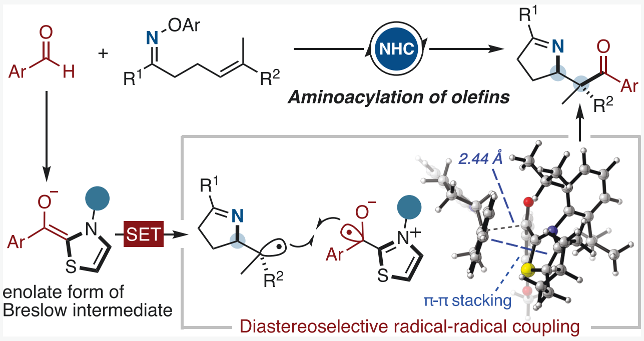

■ INTRODUCTION

Nitrogen-centered radicals are versatile reactive intermediates with broad applications in the synthesis of *N*-containing heterocycles,[1,2] which are ubiquitous structural motifs in natural products and pharmaceuticals.[3] Pre-functionalized oximes are excellent precursors for iminyl radicals owing to their weak N−O bond.[2,4] To supplement the classical methods for N−O bond cleavage via microwave[4a] (>160 °C) or UV irradiation,[4b,c] recent developments in the field of photoredox catalysis[2,5] provided an attractive way to access iminyl radicals from oxime ethers[6] and acyl oximes[7] under mild conditions (Figure 1A). These N radicals may undergo 5-*exo*-trig cyclization onto tethered alkenes, providing access to pyrrolines (Figure 1B).[6,7b] Studer and Leonori have shown, independently, that the resultant C-centered radicals could be intermolecularly captured by Michael acceptors[6b] or SOMOphiles[6c] to form C−C, C−N, and C−halide bonds. However, daunting challenges remain in the cyclization with 1,2-disubstituted alkenes, which generated a prochiral carbon-centered radical.[6a−c] The diastereoselectivity is not controlled in the following radical-involved process due to nominal interaction between the photocatalyst and radical-based intermediates, which undergo reaction with minimal activation barriers. One of the key breakthroughs in this field can be traced to a recent report by Yu and co-workers, who achieved diastereoselective imination of this type by careful selection of vinyl boronic acid as the radical acceptor.[8] In this context, the development of an appropriate catalytic system capable of controlling diastereoselectivity in radical−radical coupling reactions is highly desirable and would be of great synthetic importance. In contrast to the use of a photoredox catalyst, we envisioned that covalent-based organocatalysis could provide an opportunity to control the stereochemistry in radical-involved reactions[9] due to the strong interaction between the catalyst and the reactant.

N-Heterocyclic carbenes (NHCs) are well-known as nucleophilic organocatalysts[10] for the umpolung of aldehydes via Breslow intermediates.[11] Moving from traditional ionic chemistry logic to a radical approach, recent electrochemical[12] and methodological studies[13,14] revealed that the reduction potential of deprotonated Breslow intermediate **A** was sufficiently negative to perform single electron transfer (SET) with various single electron acceptors, such as TEMPO,[14a] nitro compounds,[14c−f] and polyhalides[14g,h] (Figure 1C). Pioneering studies from Ohmiya's group reported

Received: October 22, 2022
Published: November 24, 2022

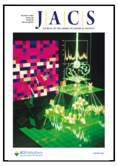

https://doi.org/10.1021/jacs.2c11209
J. Am. Chem. Soc. 2022, 144, 22767−22777

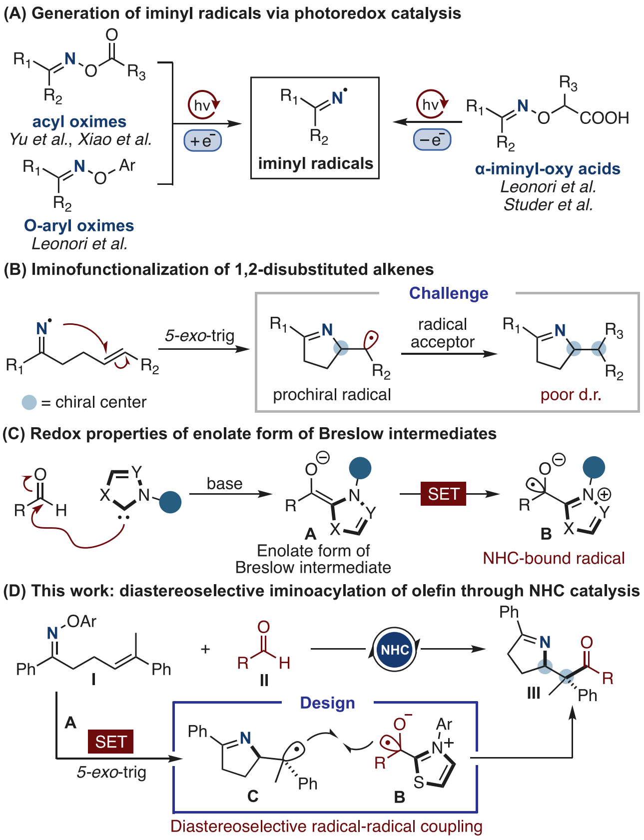

Figure 1. (A) Generation of iminyl radicals via N−O bond homolysis. (B) Access to the pyrroline derivative with vicinal stereocenters. (C) Radical NHC catalysis. (D) Diastereoselective iminoacylation of trisubstituted olefin.

NHC-catalyzed radical decarboxylative coupling of aldehydes with redox-active esters, allowing for the rapid assembly of functionalized ketones.[15] In these processes, the deprotonated Breslow intermediate **A** can serve as both a single electron donor and an acyl radical equivalent for subsequent C−C bond formation. In the past few years, the synthetic potential of NHC radical catalysis was significantly extended to a number of SET-mediated transformation processes.[16−18] It is worthwhile mentioning that this attractive strategy provides the possibility for stereocontrolled radical reactions, since the NHC catalyst is associated with the C-centered radical **B** through a covalent bond.

Herein, based on the above hypothesis, we report the development of an NHC-catalyzed process capable of generating N-centered radicals and achieving diastereoselective aminoacylation under metal- and light-free conditions. As illustrated in Figure 1D, single electron reduction of oxime ether **I** by the electron-rich Breslow intermediate **A** triggered the formation of C-centered radical **C** after 5-*exo*-trig cyclization. We envisioned that the resulting NHC-bound ketyl radical **B** could differentiate competing stereomeric transition states of the prochiral radical **C** and allow diastereoselective radical−radical coupling. This organocatalytic protocol afforded access to functionalized pyrrolines, which can be further transformed to interesting oxazinanone and indolizidine heterocycles. Moreover, we recognized an opportunity for amidyl radical generation and used them in diastereoselective amidoacylation of tethered alkenes.[2,19] Integrated experimental and computational studies revealed that the precise stereocontrol is attributed to steric hindrance on the NHC organocatalyst and $\pi-\pi$ stacking interaction between radicals **B** and **C**.

RESULTS AND DISCUSSION

Reaction Development. We envisioned a prospective catalytic cycle for the NHC-catalyzed olefin iminoacylation as shown in Figure 2. We anticipated that the deprotonated Breslow intermediate **A** would be generated from a thiazolium-type NHC and aldehyde **II** in the presence of a base. The subsequent SET event between the enolate **A** and oxime ether **I** would produce the ketyl radical **B** and iminyl radical **D** after homolysis of the N−O bond. Next, in accordance with literature precedent,[6,7b] we expected the iminyl radical **D** to perform 5-*exo*-trig cyclization to furnish a new C−N bond and the prochiral C-centered radical **C**, which would undergo diastereoselective radical cross-coupling with **B**. Finally, elimination of NHC from intermediate **E** would regenerate the organocatalyst and afford the desired pyrroline product **III** with vicinal stereocenters.

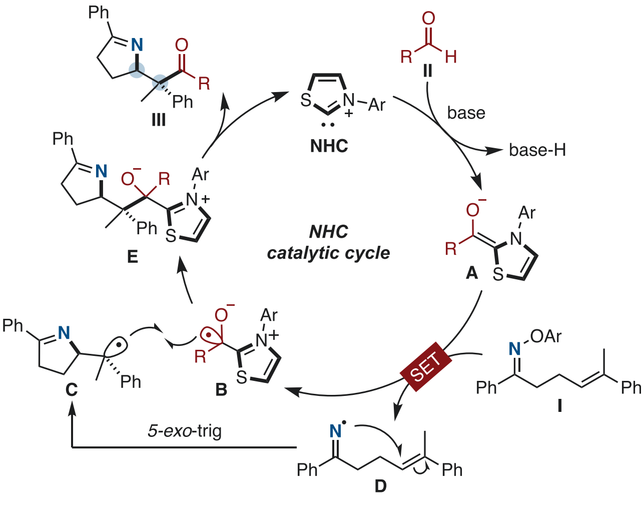

Figure 2. Prospective catalytic cycle.

Inspired by Leonori's pioneering studies on the electron-poor *O*-aryl oximes,[6a] we began our reaction condition optimization with NO_2-substituted oxime **1a** due to its ease of SET reduction (Table 1). Initially, the iminoacylation reaction with aromatic aldehyde **2** was performed in the presence of DBU and *N*-2,4,6-trimethylphenyl-substituted six-membered ring fused thiazolium salt **N1** (20 mol %). As shown in Table 1, we were pleased to find that the desired pyrroline **3** was obtained in good yield with 5:1 d.r. (entry 1). Encouraged by this result, the diastereoselective iminoacylation was evaluated by other NHC precursors. Gratifyingly, diisopropyl substituted thiazolium salt **N2** significantly improved the diastereoselectivity, furnishing **3** in 79% yield with >19:1 d.r. (Table 1, entry 2). Further investigation of the backbone moiety revealed that the seven-membered ring fused thiazolium salt **N4** was more efficient, increasing the yield to 91% as well as retaining excellent diastereoselectivity (Table 1 entry 4). The *N*-neopentyl-substituted **N5** showed comparable reactivity, but it induced lower diastereoselectivity (entry 5). Other NHCs bearing triazolium (**N6**) or imidazolium (**N7**) structures were ineffective under otherwise identical conditions (entries 6 and 7). The substituent on the *O*-aryl oxime was also

Table 1. Optimization and Control Studies[a]

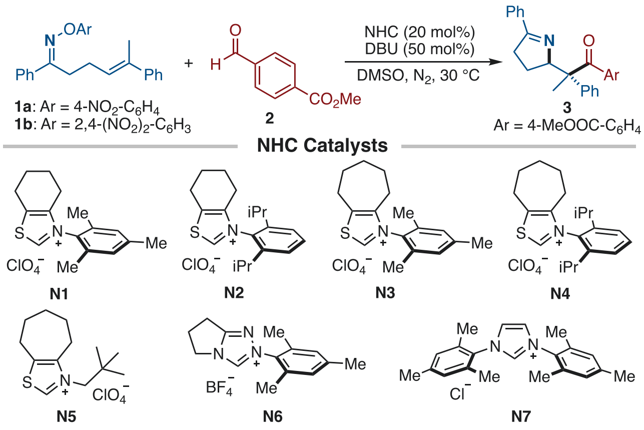

entry	NHC catalyst	solvent	yield (%)[b]	d.r.[c]
1	**N1**	DMSO	68	5:1
2	**N2**	DMSO	79	>19:1
3	**N3**	DMSO	51	5:1
4	**N4**	DMSO	91	>19:1
5	**N5**	DMSO	92	2.5:1
6	**N6**	DMSO	trace	
7	**N7**	DMSO	trace	
8[d]	**N4**	DMSO	28	>19:1
9	**N4**	DMF	68	>19:1
10	**N4**	CH_3CN	35	>19:1
11	**N4**	CH_2Cl_2	42	>19:1
12[e]	**N4**	DMSO	91	>19:1

[a] Reactions were carried out with **1a** (0.1 mmol), **2** (0.15 mmol), NHC catalyst (20 mol %), and DBU (0.5 equiv) in 1.0 mL of solvent at 30 °C for 12 h. [b] Yields of isolated products. [c] Diastereomeric ratio (d.r.) values were determined by ^{1}H NMR. [d] **1b** was used instead of **1a**. [e] 5 mol % **N4** was used.

critical for this reaction. When 2,4-dinitro-substituted aryl oxime **1b** was subjected to the reaction conditions, **3** was formed in a much lower yield (entry 8 versus entry 4). Further evaluation of the solvents led to inferior yield (entries 9−11). Pleasingly, the amount of NHC precatalyst could be reduced to 5 mol % without any loss in the yield and diastereoselectivity (entry 12).

Substrate Scope. With the optimized conditions in hand, we next explored the generality of the iminoacylation of trisubstituted alkenes. The observed excellent diastereoselectivity led us to first examine the reaction of *O*-aryl oxime **1a** with various aldehydes (Scheme 1). To our delight, the developed NHC-catalyzed radical reaction was effective over a wide range of aryl aldehydes to furnish the pyrroline products **3**−**23** in satisfying yields with excellent diastereoselectivity. It needs to be mentioned that the outcome was influenced a little by the electronic nature of the substituents on the aromatic ring. Generally, electron-deficient aryl aldehydes gave the desired products (**3**−**9**) with better yield and lower catalyst loading than the electron-rich ones (**10**−**14**). Additionally, the relative stereochemistry of the functionalized pyrroline was established by X-ray diffraction analysis of **13**. The diastereoselective transformation also proceeded smoothly with naphthyl (**17**) and various heteroaryl aldehydes such as substituted quinoline (**18**), pyridine (**19**−**21**), furan (**22**), and thiophene (**23**). In addition to aromatic aldehydes, we found that this strategy is amenable to aliphatic aldehydes (**24**−**28**) employing less sterically demanding **N5** instead of **N4**.[15c]

Notably, diverse functionalities including nitrile, thioether, alkyne, and boronic ester were all competent (**29**−**34**). The broad functional group compatibility of the reaction encouraged us to investigate its practicality for the late-stage functionalization of natural products. (−)-Menthol, estrone, and cholesterol-derived aldehydes were all compatible with the reaction conditions, providing the corresponding products (**35**−**37**) in 75−91% yield with complete diastereoselectivity. Furthermore, this iminoacylation reaction can be conducted on a gram scale, enabling the practical synthesis of pyrroline derivatives. The synthesis of pyrroline **3** and **15** was scaled up to give 1.1 gram of product in 88 and 75% yield, respectively.

Having investigated the aldehyde scope, we were interested in exploring the synthetic robustness of this diastereoselective iminoacylation reaction with other iminyl radical precursors. To this end, a variety of oxime ethers were prepared and tested with the NHC-catalyzed reaction. As shown in Scheme 2, the steric and electronic properties of the substituents on the aryl group (R_1) had a slight influence on the reaction outcomes (**38**−**44**). Fused-ring, furan, and thiophene-substituted oximes were viable substrates for producing cyclic products in good yields with >19:1 d.r. (**45**−**47**). Notably, the catalyst system was also effective with alkyl and alkenyl-based substrates (**48**−**50**). With respect to the pendant alkene moiety, a variety of trisubstituted olefins with different substitutes on the aromatic ring (R_2) were successfully accommodated (**51**−**56**). For the substrates containing disubstituted olefin (**58**), diastereoselectivity was low due to enolized racemization.[20] Dimethyl substituted alkene could also be used as an acceptor, albeit with a lower yield for the target **59**. Unfortunately, oxime with a terminal double bond (**60**) was not successful, presumably due to the instability of the primary radical generated by cyclization. In addition, oxime substrates that contain *gem*-dimethyl substituents at the alpha-position of the C=N double bond (R_4 = R_5 = Me), worked smoothly to deliver product **61** in high yield. When tetralin oxime was used, tricyclic product **62** was obtained in 84% yield, albeit with lower diastereoselectivity.

Synthetic Applications. To further demonstrate the synthetic utility of this reaction, the conversion of product **15** into various derivatives was examined. As shown in Scheme 3, the functionalized pyrroline derivative **15** can further participate in several carbonyl-based transformations, including the Wittig reaction to form alkene **63**, and Baeyer−Villiger oxidation to afford carboxylic ester **64**. Hydrogenation of the imine offers opportunities to generate pyrrolidine derivatives. The pyrrolidine derivative **65** could be converted into 3-amino alcohol **67** under reductive conditions. Cyclization of **67** with 1,1′-carbonyldiimidazole (CDI) in THF at reflux temperature gave the 1,3-oxazinan-2-one derivative **68** in 84% yield without any loss of diastereoselectivity. The structure of cycloadduct **68** was unambiguously confirmed by an X-ray crystallographic analysis. Furthermore, acylation of **65** followed by the ring-closing Wittig reaction yielded the indolizidine derivative **70**, which is an important framework of many natural products.[21]

Experimental Investigations on the Reaction Pathways. Upon exploration of the diastereoselective iminoacylation to display a broad scope and high synthetic applicability, we were encouraged to investigate mechanistic details (Scheme 4). In order to investigate the redox properties of Breslow-type derivatives, a series of acyl thiazoliums **F** were synthesized for cyclic voltammetry studies.[12d,22] As shown in Scheme 4A, scan of **F1** in CH_3CN containing 0.1 M nBu$_4$NPF$_6$ produced two

Scheme 1. Scope of Aldehydes[a]

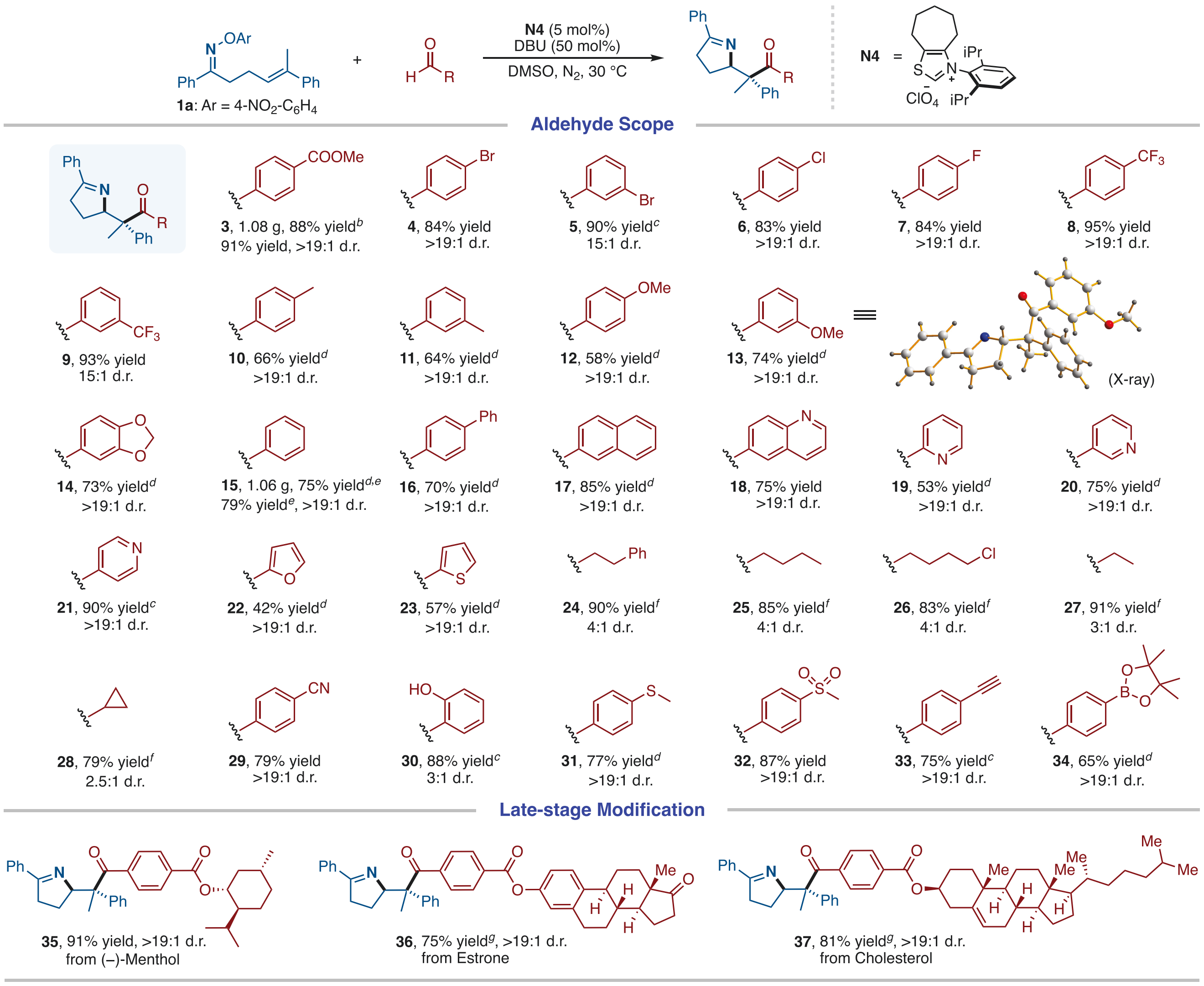

[a] Reaction conditions: *O*-aryl oxime **1a** (0.1 mmol), aldehyde (1.5 equiv), NHC precatalyst **N4** (5 mol %), DBU (50 mol %) in DMSO (1.0 mL) at 30 °C for 12 h. Isolated product yields. Diastereomeric ratio (d.r.) values were determined by ^{1}H NMR. [b] 3.0 mmol of **1a** was used. [c] 10 mol % of catalyst was used. [d] 20 mol % of catalyst was used. [e] 4.0 mmol of **1a** was used. [f] Reaction was performed with NHC precatalyst **N5** (20 mol %) and Cs_2CO_3 (50 mol %) at 60 °C. [g] Reaction was performed in DMSO/CH_2Cl_2 (4.0 mL, v/v = 1:1).

successive reversible reduction waves. It features a reversible first reduction wave at $E^1_{1/2}$ = −0.53 V versus SCE, which corresponds to the reduction of **F1** to ketyl radical **B1**. Importantly, further single-electron reduction of persistent radical **B1** afforded enolate **A1** with significantly lower potentials ($E^2_{1/2}$[**B1**/**A1**] = −1.32 V vs SCE). The electronic properties of the substituents on the aryl group had a slight influence on the reduction potentials ($E^2_{1/2}$[**B2**/**A2**] = −1.36 V vs SCE; $E^2_{1/2}$[**B3**/**A3**] = −1.29 V vs SCE). These results highlight the strong reducing ability of Breslow-type derivatives, thus making the ground-state SET with oxime ether **1a** ($E_{p/2}$ [**1a**/**1a**$^{\cdot-}$] = −1.04 V vs SCE) exergonic ($\Delta G_{SET} \approx -5$ kcal mol^{-1}).[23,24]

To further probe the involvement of NHC-bound ketyl radical **B**, a chiral NHC precatalyst **N8**[16f] was tested under the reaction conditions (Scheme 4B). We envisioned this may facilitate the enantioselective iminoacylation of olefins. However, the coupling product **3** was obtained as a racemic mixture (eq 1), presumably due to the influence of a racemic stereocenter in the coupling partner **C**.[25] Thus, we prepared oxime **71**, and tested it with benzaldehyde and **N8** (eq 2). In this case, we proposed that the iminyl radical would undergo intramolecular 1,5-hydrogen atom abstraction (HAT) rather than cyclization, delivering the acyclic radical **G**.[2c,g] As the result, 1,5-dione **72** was isolated with 16% ee. This outcome supports our hypothesis of the formation of the NHC-bound ketyl radical **B** and its participation in the radical−radical coupling step. Meanwhile, a radical trapping experiment was conducted (Scheme 4C). In the presence of 3.0 equiv of PhSeSePh, the standard reaction of **1a** and **2** furnished the selenide **73** in 63% yield. Moreover, oxime ether **74**, which bears a 2-phenylcyclopropyl group, was synthesized as a radical clock (Scheme 4D). In this event, the NHC-catalyzed reaction gave the expected fragmentation product **75** as a mixture of diastereomers. Pleasingly, two of the isomers were isolated in 30% yield and fully characterized, which provided strong support for the formation of the C-centered radical **C**.

Scheme 2. Scope of Oximes[a]

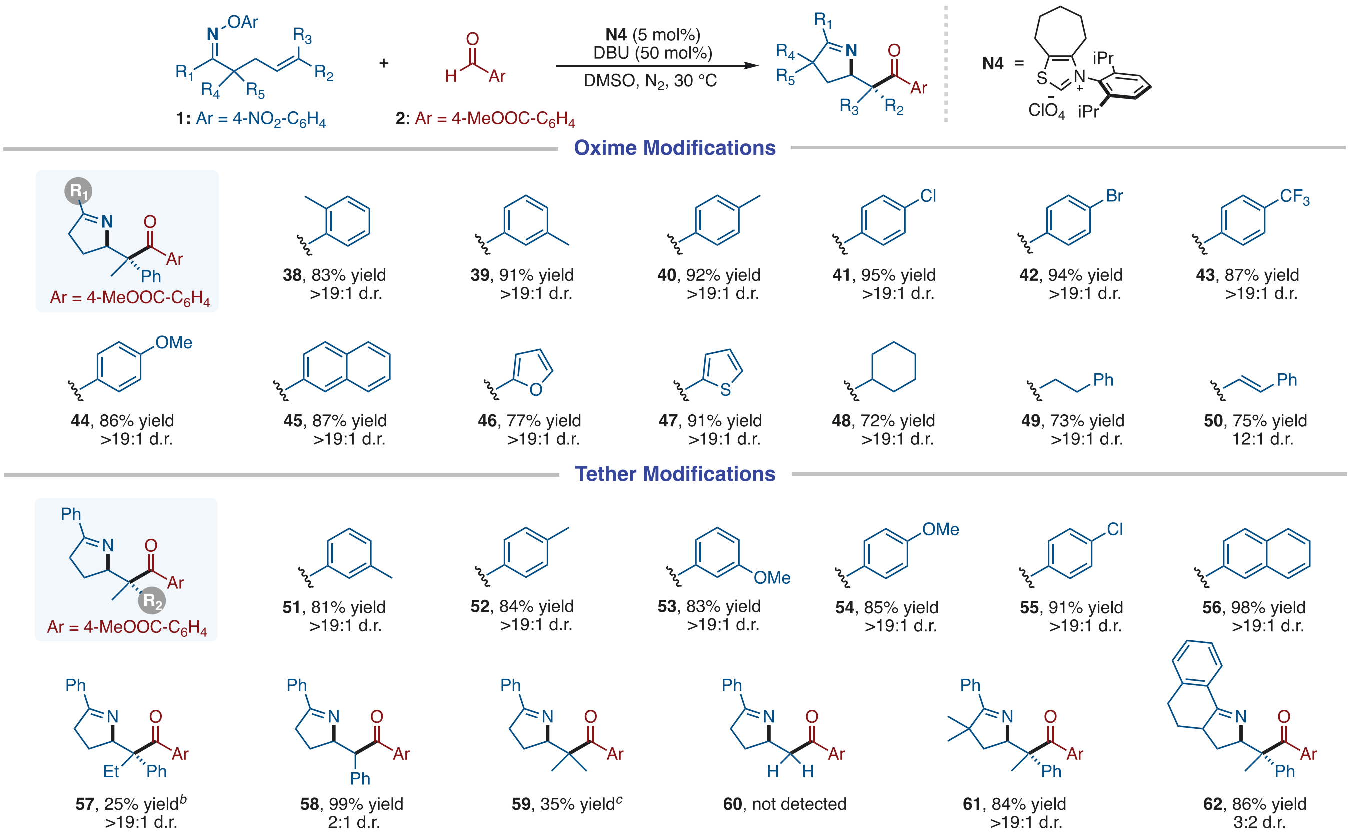

[a] See Scheme 1 and SI for detailed procedures. Isolated yields. Diastereomeric ratio (d.r.) values were determined by ^{1}H NMR. [b] 20 mol % of catalyst was used. [c] 50 mol % of Cs_2CO_3 was used instead of DBU.

Scheme 3. Synthetic Transformations of 9[a]

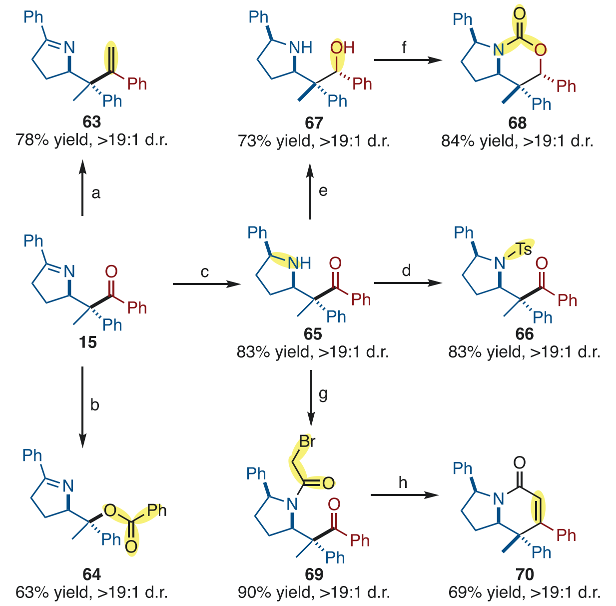

[a] Reaction conditions: (a) PPh_3CH_3Br, *n*-BuLi, THF, −78 °C to r.t.; (b) *m*-CPBA, $NaHCO_3$, CH_2Cl_2, r.t.; (c) 10% Pd/C, H_2 (1 atm.), EtOAc, r.t.; (d) TsCl, Et_3N, CH_2Cl_2, r.t.; (e) $NaBH_4$, MeOH, 0 °C to r.t.; (f) CDI, THF, reflux; (g) bromoacetyl bromide, Et_3N, CH_2Cl_2, 0 °C to r.t.; and (h) PPh_3, THF, r.t., then NaH, THF.

Computational Studies. To better understand the mechanistic details, energy profiles of the proposed pathways were evaluated by density functional theory (DFT) calculations (Scheme 5). Addition of NHC catalyst **N4′** to *m*-anisaldehyde **13′** occurs via **TS1** (21.0 kcal/mol) to form **INT1**, which is further deprotonated by DBU to form Breslow intermediate **INT2** and DBU-H$^+$. Oxime **1a** and Breslow intermediate **INT2** undergo SET to generate reduced oxime **INT3** and oxidized Breslow intermediate **INT4**. Then, fragmentation occurs from the radical anion of oxime **INT3** to produce N-radical intermediate **INT7** and phenoxide **INT5** that forms phenol **INT6** by protonation with DBU-H$^+$. N-radical intermediate **INT7** cyclizes via **TS2** (−11.2 kcal/mol) in order to form cyclized radical intermediate **INT8.** Oxidized Breslow intermediate **INT4**, which was generated by SET, undergoes coupling with cyclized radical intermediate **INT8** via **TS3** (−15.9 kcal/mol) to produce coupling intermediate **INT9**. NHC elimination via **TS4** (−21.7 kcal/mol) from intermediate **INT9** generates product and regenerates NHC catalyst **N4′**. The overall reaction progress is exergonic by 50.1 kcal/mol. Based on the computational results, the radical coupling step is the rate-determining step. While radical coupling often occurs with very low barriers, both of these radicals are stabilized and sterically hindered.

Since the radical coupling step is the rate-determining step, cyclized radical intermediate **INT8** or oxidized Breslow intermediate **INT4**[26] can be trapped by radical traps such as PhSeSePh. As shown in Scheme 4C, experimental mechanistic studies observed radical trapping of cyclized radical intermediate **INT8** by PhSeSePh. Both computational and

https://doi.org/10.1021/jacs.2c11209
J. Am. Chem. Soc. 2022, 144, 22767−22777

Scheme 4. (A–D) Experimental Mechanistic Studies

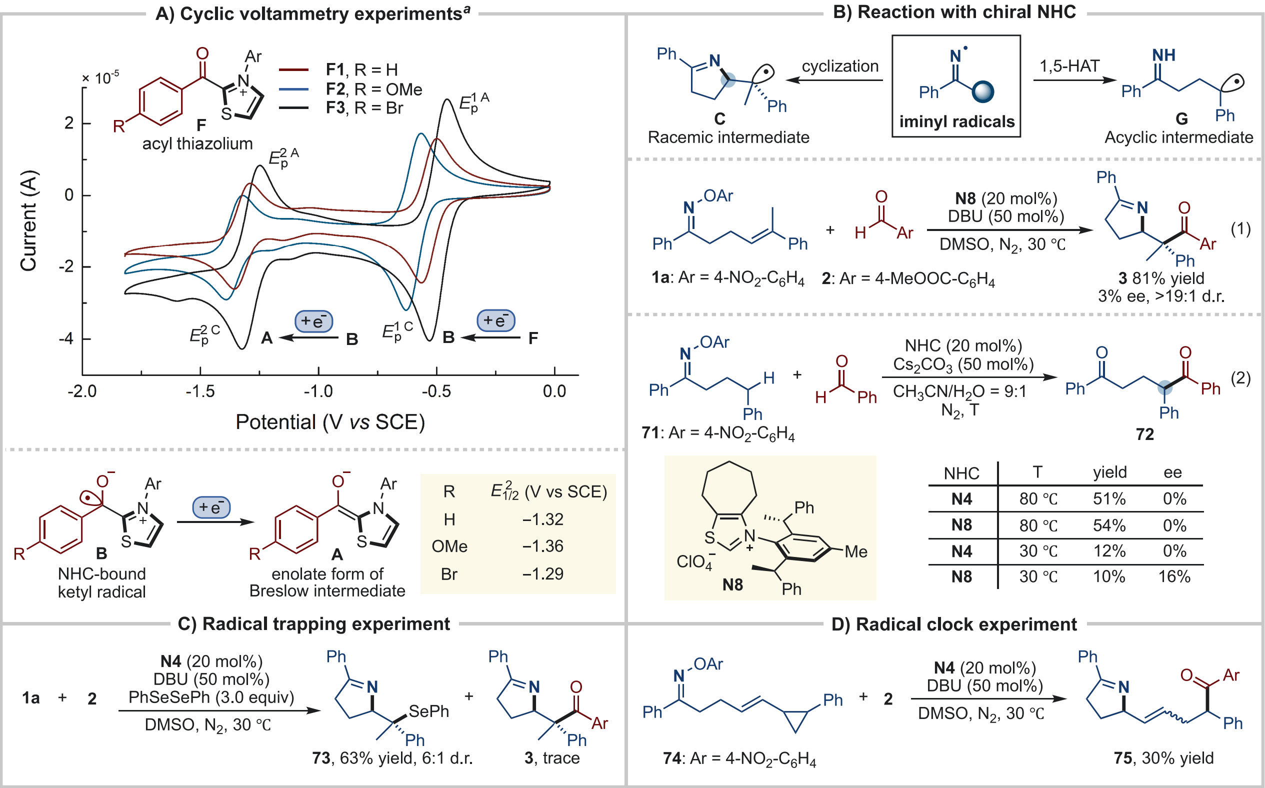

R	$E^2_{1/2}$ (V vs SCE)
H	−1.32
OMe	−1.36
Br	−1.29

NHC	T	yield	ee
N4	80 °C	51%	0%
N8	80 °C	54%	0%
N4	30 °C	12%	0%
N8	30 °C	10%	16%

[a] Cyclic voltammetry of 1 mM **F** in CH_3CN with 0.1 M nBu_4NPF_6 electrolyte at a 100 mVs^{-1} rate. Each voltammogram was obtained independently.

experimental studies support that the rate-determining step is the radical coupling step.

In addition to describing the overall reaction pathway, we explored the origin of diastereoselectivity in radical coupling. We found **TS3**, which forms the experimental product that is confirmed by X-ray crystallography, and **TS3′** forming its diastereomer (Scheme 5). **TS3** is favored by 1.5 kcal/mol compared to **TS3′**, which is close to the experimental outcome (>19:1 d.r., approximately 1.7 kcal/mol). We think that the energy difference between **TS3** and **TS3′** is caused by favorable $\pi-\pi$ interactions, likely mainly dispersive attraction between the phenyl of the cumene substructure and thiazole of the NHC substructure in **TS3** (Scheme 5C). In contrast to **TS3**, $\pi-\pi$ interactions are not involved in **TS3′** (Scheme 5E). **TS3′** is a perfectly staggered conformation as is generally favorable, but **TS3** can bring the two aromatics into appropriate attractive distances. For the validation of our hypothesis of $\pi-\pi$ interaction involvement in the diastereoselectivity-determining step, we conducted single-point calculations of **TS3a** and **TS3a′** with the phenyl substituent replaced by H (Scheme 5D). Here, **TS3a** became disfavored by 1.4 kcal/mol due to the unfavorable eclipsed structure. It shows that the role of $\pi-\pi$ interactions by the phenyl substituent is important to control the selectivity. Thus, we suggest that $\pi-\pi$ interactions contribute to lowering the energy of **TS3** relative to **TS3′**.

Further Classes of Reactivity. Building on the mechanistic understanding of this NHC-catalyzed radical reaction, we decided to evaluate whether this strategy could be applied to the generation of amidyl radicals. Gratifyingly, the diastereoselective amidoacylation of olefins was achieved (Scheme 6). We hypothesized that electron-poor aryloxy-amide **76a** (R = Ph, $E_{1/2}$ = −0.97 V vs SCE) would be an ideal amidyl radical precursor.[19b,d] Upon SET reduction and homolysis of the N–O bond, the amidyl radical **H** is expected to undergo 5-*exo*-trig cyclization. The resultant C-centered radical **I** subsequently engages in radical–radical coupling with **B** to form the desired oxazolidinone derivative and regenerate the NHC catalyst. We anticipated that the NHC-bound ketyl radical **B** would differentiate the stereochemistry of **I**, affording the cyclic carbamate with excellent diastereoselectivity.

The desired transformation was feasible to afford the coupling product by employing reaction conditions similar to the ones presented above. However, we realized that the amidyl radical may undergo HAT to provide the amide byproduct **77** owing to its electrophilic nature.[27] This competing pathway led to a decrease in the formation of amidoacylation products. Scope investigation demonstrated that a series of aldehydes bearing electron-rich or electron-deficient groups at the para- and meta-positions were compatible with the reaction, giving **78**–**90** in good yields. Additionally, the oxazolidinone **91** generated from 2-naphthaldehyde afforded a single crystal, enabling X-ray structure determination to confirm the relative stereochemistry.[28] In regard to the R on the alkene moiety in **76**, several phenyl rings were applicable to the reaction. Importantly, we obtained oxazolidinone derivatives with excellent diastereoselectivity, further demonstrating the significance of this organocatalytic system.

Scheme 5. (A–E) Computational Mechanistic Studies[a]

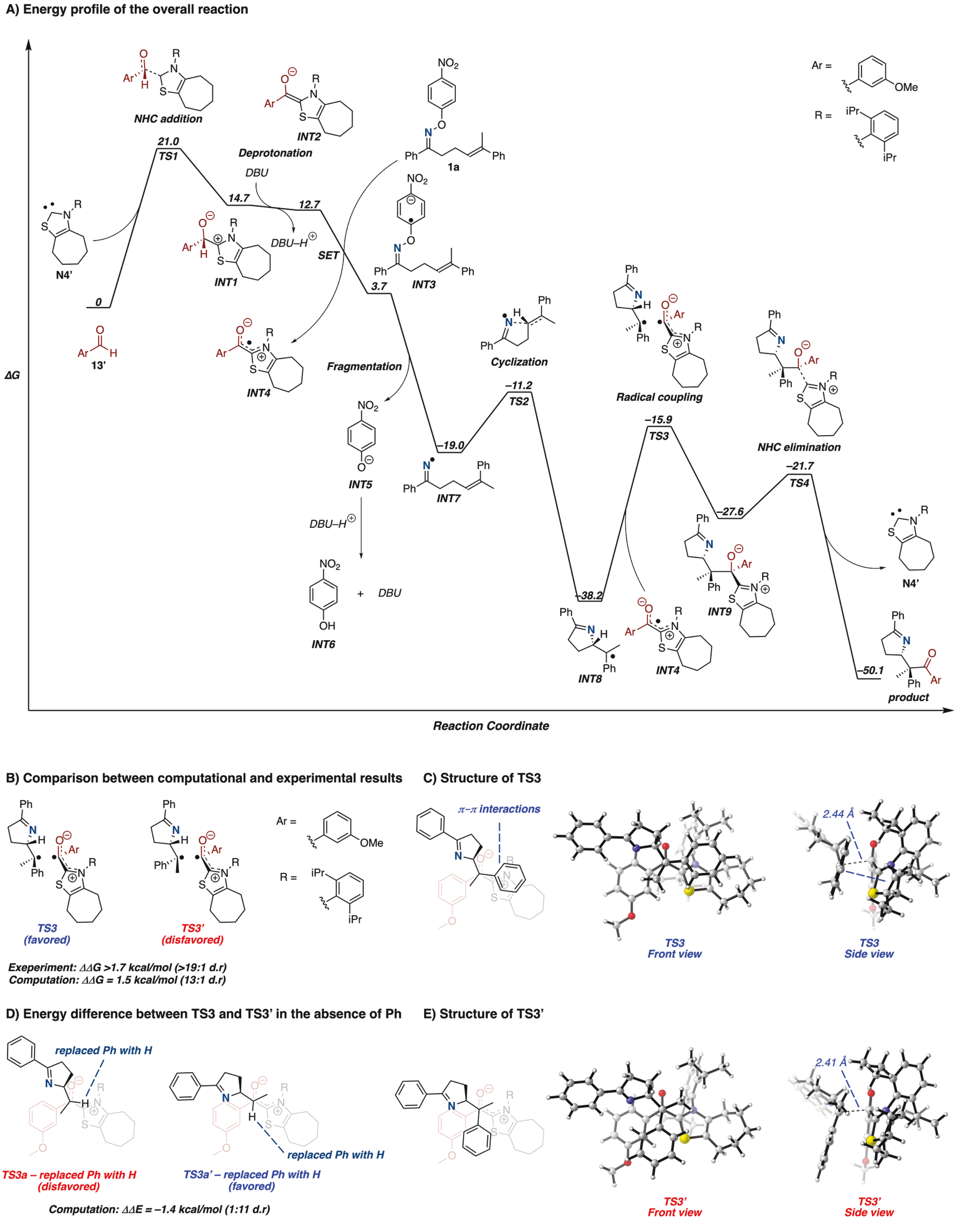

[a] Computational studies are performed with (u)ωB97X-D/def2-tzvpp/SMD=DMSO//(u)ωB97X-D/def2-svp/SMD=DMSO at 298.15 K. The unit of Gibbs free energies is kcal/mol.

Scheme 6. Diastereoselective Amidoacylation of Olefins[a]

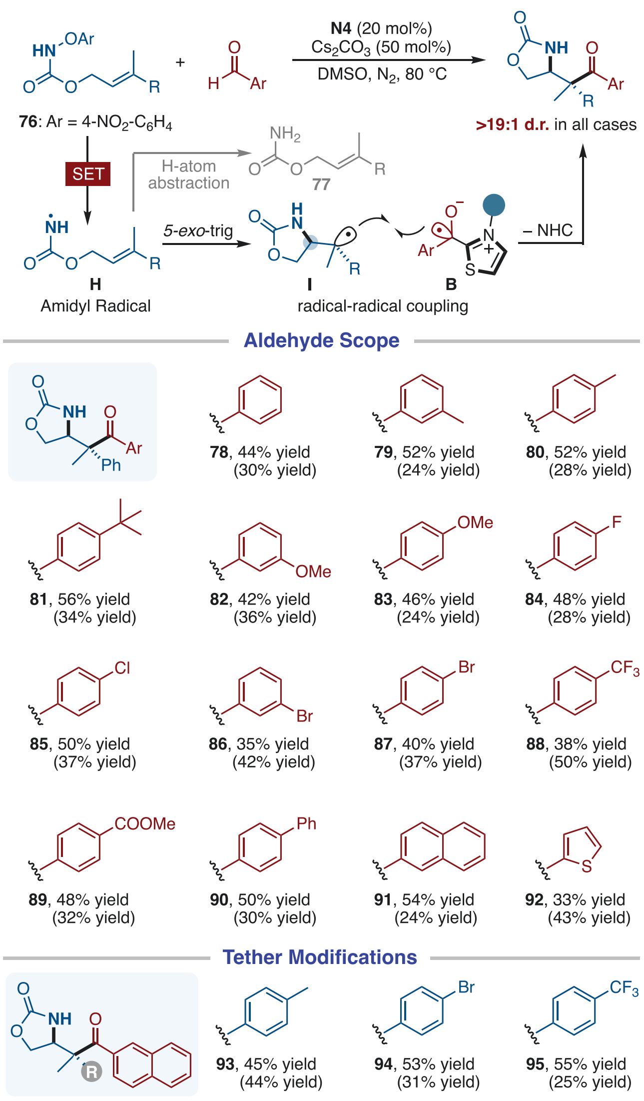

[a]Reaction conditions: *O*-aryl carbamate **76** (0.2 mmol), aldehyde (1.5 equiv), NHC precatalyst **N4** (20 mol %), Cs_2CO_3 (50 mol %) in DMSO (2.0 mL) at 80 °C for 12 h. Isolated product yields. Diastereomeric ratio (d.r.) values were determined by ^1H NMR. Yields of the amide byproduct are given in parentheses.

■ CONCLUSIONS

In summary, we have developed a synthetic method for the diastereoselective iminoacylation and amidoacylation of trisubstituted alkenes under covalent-based NHC radical catalysis. Central to the success of this strategy is the formation of a thiazolium-derived Breslow intermediate with proper sterics, which not only promotes single-electron transfer but also controls the diastereoselectivity. This approach provides ready access to functionalized pyrrolines, which are easily elaborated to the synthesis of pyrrolidines. The combined experimental and computational investigations of this organocatalytic system provide an understanding of how diastereoselective radical−radical coupling occurs and suggest that the radical coupling step is the diastereoselectivity- and rate-determining step. A series of acyl thiazoliums, the most oxidized Breslow-type derivatives, were synthesized for cyclic voltammetry studies, indicating redox potentials as negative as −1.36 V versus SCE. Further application of this strategy to enantioselective radical-involved transformations is anticipated in view of the tremendous success of chiral NHC in asymmetric organocatalysis.

■ ASSOCIATED CONTENT

Supporting Information

The Supporting Information is available free of charge at https://pubs.acs.org/doi/10.1021/jacs.2c11209.

Experimental procedures and analytical data (PDF)

Accession Codes

CCDC 2155949, 2161395, and 2205064 contain the supplementary crystallographic data for this paper. These data can be obtained free of charge via www.ccdc.cam.ac.uk/data_request/cif, or by emailing data_request@ccdc.cam.ac.uk, or by contacting The Cambridge Crystallographic Data Centre, 12 Union Road, Cambridge CB2 1EZ, UK; fax: +44 1223 336033.

■ AUTHOR INFORMATION

Corresponding Authors

Kendall N. Houk − *Department of Chemistry and Biochemistry, University of California, California, Los Angeles 90095-1569, United States*; orcid.org/0000-0002-8387-5261; Email: houk@chem.ucla.edu

Jiannan Zhao − *Zhang Dayu School of Chemistry, Dalian University of Technology, Dalian 116024, P. R. China*; orcid.org/0000-0002-5546-7383; Email: jnzhao@dlut.edu.cn

Authors

Wen-Deng Liu − *Zhang Dayu School of Chemistry, Dalian University of Technology, Dalian 116024, P. R. China*

Woojin Lee − *Department of Chemistry and Biochemistry, University of California, California, Los Angeles 90095-1569, United States*

Hanyu Shu − *Zhang Dayu School of Chemistry, Dalian University of Technology, Dalian 116024, P. R. China*

Chuyu Xiao − *Zhang Dayu School of Chemistry, Dalian University of Technology, Dalian 116024, P. R. China*

Huiwei Xu − *Zhang Dayu School of Chemistry, Dalian University of Technology, Dalian 116024, P. R. China*

Xiangyang Chen − *Department of Chemistry and Biochemistry, University of California, California, Los Angeles 90095-1569, United States*; orcid.org/0000-0002-6981-7022

Complete contact information is available at: https://pubs.acs.org/10.1021/jacs.2c11209

Author Contributions

§W.-D.L. and W.L. contributed equally to this paper.

Notes

The authors declare no competing financial interest.

■ ACKNOWLEDGMENTS

J.Z. is grateful for the financial support provided by the National Natural Science Foundation of China (No. 21901030) and the Fundamental Research Funds for the Central Universities (No. DUT22LK25). K.N.H. is grateful to the National Science Foundation (CHE-1764328) for the financial support of this research. Computations were performed on the UCLA Institute of Digital Research and Education Hoffman2 Cluster. We thank Yuqiao Zhou (Sichuan

University) and Haiyu Zhou (Dalian University of Technology) for the X-ray crystallography data collection and analysis.

■ REFERENCES

(1) For selected reviews, see: (a) Kitamura, M.; Narasaka, K. Catalytic Radical Cyclization of Oximes Induced by One-Electron Transfer. *Bull. Chem. Soc. Jpn.* **2008**, *81*, 539−547. (b) Zard, S. Z. Recent Progress in the Generation and Use of Nitrogen-Centred Radicals. *Chem. Soc. Rev.* **2008**, *37*, 1603−1618. (c) Walton, J. C. The Oxime Portmanteau Motif: Released Heteroradicals Undergo Incisive EPR Interrogation and Deliver Diverse Heterocycles. *Acc. Chem. Res.* **2014**, *47*, 1406−1416. (d) Walton, J. C. Functionalised Oximes: Emergent Precursors for Carbon-, Nitrogen- and Oxygen-Centred Radicals. *Molecules* **2016**, *21*, 63.

(2) For recent reviews, see: (a) Chen, J.-R.; Hu, X.-Q.; Lu, L.-Q.; Xiao, W.-J. Visible Light Photoredox-Controlled Reactions of N-Radicals and Radical Ions. *Chem. Soc. Rev.* **2016**, *45*, 2044−2056. (b) Xiong, T.; Zhang, Q. New Amination Strategies Based on Nitrogen-Centered Radical Chemistry. *Chem. Soc. Rev.* **2016**, *45*, 3069−3087. (c) Davies, J.; Morcillo, S. P.; Douglas, J. J.; Leonori, D. Hydroxylamine Derivatives as Nitrogen-Radical Precursors in Visible-Light Photochemistry. *Chem. − Eur. J.* **2018**, *24*, 12154−12163. (d) Jiang, H.; Studer, A. Chemistry With N-Centered Radicals Generated by Single-Electron Transfer-Oxidation Using Photoredox Catalysis. *CCS Chem.* **2019**, *1*, 38−49. (e) Yu, X.-Y.; Zhao, Q.-Q.; Chen, J.; Xiao, W.-J.; Chen, J.-R. When Light Meets Nitrogen-Centered Radicals: From Reagents to Catalysts. *Acc. Chem. Res.* **2020**, *53*, 1066−1083. (f) Song, C.; Shen, X.; Yu, F.; He, Y.; Yu, S. Generation and Application of Iminyl Radicals from Oxime Derivatives Enabled by Visible Light Photoredox Catalysis. *Chin. J. Org. Chem.* **2020**, *40*, 3748−3759. (g) Kwon, K.; Simons, R. T.; Nandakumar, M.; Roizen, J. L. Strategies to Generate Nitrogen-Centered Radicals That May Rely on Photoredox Catalysis: Development in Reaction Methodology and Applications in Organic Synthesis. *Chem. Rev.* **2022**, *122*, 2353−2428. (h) Pratley, C.; Fenner, S.; Murphy, J. A. Nitrogen-Centered Radicals in Functionalization of sp^2 Systems: Generation, Reactivity, and Applications in Synthesis. *Chem. Rev.* **2022**, *122*, 8181−8260.

(3) (a) Welsch, M. E.; Snyder, S. A.; Stockwell, B. R. Privileged Scaffolds for Library Design and Drug Discovery. *Curr. Opin. Chem. Biol.* **2010**, *14*, 347−361. (b) Vitaku, E.; Smith, D. T.; Njardarson, J. T. Analysis of the Structural Diversity, Substitution Patterns, and Frequency of Nitrogen Heterocycles among U.S. FDA Approved Pharmaceuticals. *J. Med. Chem.* **2014**, *57*, 10257−10274.

(4) For recent selected examples, see: (a) Markey, S. J.; Lewis, W.; Moody, C. J. A New Route to α-Carbolines Based on 6π-Electrocyclization of Indole-3-alkenyl Oximes. *Org. Lett.* **2013**, *15*, 6306−6308. (b) Mikami, T.; Narasaka, K. Photochemical Transformation of γ,δ-Unsaturated Ketone *O*-(*p*-Cyanophenyl)oximes to 3,4-Dihydro-2*H*-pyrrole Derivatives. *Chem. Lett.* **2000**, *29*, 338−339. (c) McBurney, R. T.; Walton, J. C. Dissociation or Cyclization: Options for a Triad of Radicals Released from Oxime Carbamates. *J. Am. Chem. Soc.* **2013**, *135*, 7349−7354.

(5) For selected reviews, see: (a) Narayanam, J. M. R.; Stephenson, C. R. J. Visible Light Photoredox Catalysis: Applications in Organic Synthesis. *Chem. Soc. Rev.* **2011**, *40*, 102−113. (b) Prier, C. K.; Rankic, D. A.; MacMillan, D. W. C. Visible Light Photoredox Catalysis with Transition Metal Complexes: Applications in Organic Synthesis. *Chem. Rev.* **2013**, *113*, 5322−5363. (c) Skubi, K. L.; Blum, T. R.; Yoon, T. P. Dual Catalysis Strategies in Photochemical Synthesis. *Chem. Rev.* **2016**, *116*, 10035−10074.

(6) (a) Davies, J.; Booth, S. G.; Essafi, S.; Dryfe, R. A. W.; Leonori, D. Visible-Light-Mediated Generation of Nitrogen-Centered Radicals: Metal-Free Hydroimination and Iminohydroxylation Cyclization Reactions. *Angew. Chem., Int. Ed.* **2015**, *54*, 14017−14021. (b) Jiang, H.; Studer, A. Iminyl-Radicals by Oxidation of α-Iminooxy Acids: Photoredox-Neutral Alkene Carboimination for the Synthesis of Pyrrolines. *Angew. Chem., Int. Ed.* **2017**, *56*, 12273−12276. (c) Davies, J.; Sheikh, N. S.; Leonori, D. Photoredox Imino Functionalizations of Olefins. *Angew. Chem., Int. Ed.* **2017**, *56*, 13361−13365. (d) Usami, K.; Yamaguchi, E.; Tada, N.; Itoh, A. Visible-Light-Mediated Iminyl Radical Generation from Benzyl Oxime Ether: Synthesis of Pyrroline via Hydroimination Cyclization. *Org. Lett.* **2018**, *20*, 5714−5717.

(7) (a) Jiang, H.; An, X.; Tong, K.; Zheng, T.; Zhang, Y.; Yu, S. Visible-Light-Promoted Iminyl-Radical Formation from Acyl Oximes: A Unified Approach to Pyridines, Quinolines, and Phenanthridines. *Angew. Chem., Int. Ed.* **2015**, *54*, 4055−4059. (b) Cai, S.-H.; Xie, J.-H.; Song, S.; Ye, L.; Feng, C.; Loh, T.-P. Visible-Light-Promoted Carboimination of Unactivated Alkenes for the Synthesis of Densely Functionalized Pyrroline Derivatives. *ACS Catal.* **2016**, *6*, 5571−5574. (c) Shu, W.; Nevado, C. Visible-Light-Mediated Remote Aliphatic C−H Functionalizations through a 1,5-Hydrogen Transfer Cascade. *Angew. Chem., Int. Ed.* **2017**, *56*, 1881−1884. (d) Yu, X.-Y.; Chen, J.-R.; Wang, P.-Z.; Yang, M.-N.; Liang, D.; Xiao, W.-J. A Visible-Light-Driven Iminyl Radical-Mediated C−C Single Bond Cleavage/Radical Addition Cascade of Oxime Esters. *Angew. Chem., Int. Ed.* **2018**, *57*, 738−743.

(8) Shen, X.; Huang, C.; Yuan, X.-A.; Yu, S. Diastereoselective and Stereodivergent Synthesis of 2-Cinnamylpyrrolines Enabled by Photoredox-Catalyzed Iminoalkenylation of Alkenes. *Angew. Chem., Int. Ed.* **2021**, *60*, 9672−9679.

(9) Leifert, D.; Studer, A. The Persistent Radical Effect in Organic Synthesis. *Angew. Chem., Int. Ed.* **2020**, *59*, 74−108.

(10) For selected reviews, see: (a) Enders, D.; Niemeier, O.; Henseler, A. Organocatalysis by N-Heterocyclic Carbenes. *Chem. Rev.* **2007**, *107*, 5606−5655. (b) Hopkinson, M. N.; Richter, C.; Schedler, M.; Glorius, F. An Overview of N-Heterocyclic Carbenes. *Nature* **2014**, *510*, 485−496. (c) Flanigan, D. M.; Romanov-Michailidis, F.; White, N. A.; Rovis, T. Organocatalytic Reactions Enabled by N-Heterocyclic Carbenes. *Chem. Rev.* **2015**, *115*, 9307−9387. (d) Wang, M. H.; Scheidt, K. A. Cooperative Catalysis and Activation with N-Heterocyclic Carbenes. *Angew. Chem., Int. Ed.* **2016**, *55*, 14912−14922. (e) Chen, X.-Y.; Gao, Z.-H.; Ye, S. Bifunctional N-Heterocyclic Carbenes Derived from L-Pyroglutamic Acid and Their Applications in Enantioselective Organocatalysis. *Acc. Chem. Res.* **2020**, *53*, 690−702. (f) Chen, X.; Wang, H.; Jin, Z.; Chi, Y. R. N-Heterocyclic Carbene Organocatalysis: Activation Modes and Typical Reactive Intermediates. *Chin. J. Chem.* **2020**, *38*, 1167−1202.

(11) (a) Breslow, R. On the Mechanism of Thiamine Action. IV. Evidence from Studies on Model Systems. *J. Am. Chem. Soc.* **1958**, *80*, 3719−3726. (b) Enders, D.; Niemeier, O.; Balensiefer, T. Asymmetric Intramolecular Crossed-Benzoin Reactions by N-Heterocyclic Carbene Catalysis. *Angew. Chem., Int. Ed.* **2006**, *45*, 1463−1467.

(12) (a) Nakanishi, I.; Itoh, S.; Suenobu, T.; Fukuzumi, S. Electron Transfer Properties of Active Aldehydes Derived from Thiamin Coenzyme Analogues. *Chem. Commun.* **1997**, 1927−1928. (b) Nakanishi, I.; Itoh, S.; Suenobu, T.; Fukuzumi, S. Direct Observation of Radical Intermediates While Investigating the Redox Behavior of Thiamin Coenzyme Models. *Angew. Chem., Int. Ed.* **1998**, *37*, 992−994. (c) Nakanishi, I.; Itoh, S.; Fukuzumi, S. Electron-Transfer Properties of Active Aldehydes of Thiamin Coenzyme Models, and Mechanism of Formation of the Reactive Intermediates. *Chem. − Eur. J.* **1999**, *5*, 2810−2818. (d) Delfau, L.; Nichilo, S.; Molton, F.; Broggi, J.; Tomás-Mendivil, E.; Martin, D. Critical Assessment of the Reducing Ability of Breslow-type Derivatives and Implications for Carbene-Catalyzed Radical Reactions. *Angew. Chem., Int. Ed.* **2021**, *60*, 26783−26789.

(13) For selected reviews on NHC radical catalysis, see: (a) Ishii, T.; Nagao, K.; Ohmiya, H. Recent Advances in N-Heterocyclic Carbene-based Radical Catalysis. *Chem. Sci.* **2020**, *11*, 5630−5636. (b) Ohmiya, H. N-Heterocyclic Carbene-Based Catalysis Enabling Cross-Coupling Reactions. *ACS Catal.* **2020**, *10*, 6862−6869. (c) Dai, L.; Ye, S. Recent Advances in N-Heterocyclic Carbene-Catalyzed Radical Reactions. *Chin. Chem. Lett.* **2021**, *32*, 660−667. (d) Li, Q.-Z.; Zeng, R.; Han, B.; Li, J.-L. Single-Electron Transfer Reactions Enabled by N-Heterocyclic Carbene Organocatalysis. *Chem. − Eur. J.* **2021**,

27, 3238−3250. (e) Liu, K.; Schwenzer, M.; Studer, A. Radical NHC Catalysis. *ACS Catal.* **2022**, *12*, 11984−11999.

(14) (a) Guin, J.; De Sarkar, S.; Grimme, S.; Studer, A. Biomimetic Carbene-Catalyzed Oxidations of Aldehydes Using TEMPO. *Angew. Chem., Int. Ed.* **2008**, *47*, 8727−8730. (b) De Sarkar, S.; Grimme, S.; Studer, A. NHC Catalyzed Oxidations of Aldehydes to Esters: Chemoselective Acylation of Alcohols in Presence of Amines. *J. Am. Chem. Soc.* **2010**, *132*, 1190−1191. (c) White, N. A.; Rovis, T. Enantioselective N-Heterocyclic Carbene-Catalyzed *β*-Hydroxylation of Enals Using Nitroarenes: An Atom Transfer Reaction That Proceeds via Single Electron Transfer. *J. Am. Chem. Soc.* **2014**, *136*, 14674−14677. (d) White, N. A.; Rovis, T. Oxidatively Initiated NHC-Catalyzed Enantioselective Synthesis of 3,4-Disubstituted Cyclopentanones from Enals. *J. Am. Chem. Soc.* **2015**, *137*, 10112−10115. (e) Li, B.-S.; Wang, Y.; Proctor, R. S. J.; Zhang, Y.; Webster, R. D.; Yang, S.; Song, B.; Chi, Y. R. Carbene-Catalysed Reductive Coupling of Nitrobenzyl Bromides and Activated Ketones or Imines via Single-Electron-Transfer Process. *Nat. Commun.* **2016**, *7*, 12933−12940. (f) Chen, X.-Y.; Chen, K.-Q.; Sun, D.-Q.; Ye, S. N-Heterocyclic Carbene-Catalyzed Oxidative [3 + 2] Annulation of Dioxindoles and Enals: Cross Coupling of Homoenolate and Enolate. *Chem. Sci.* **2017**, *8*, 1936−1941. (g) Yang, W.; Hu, W.; Dong, X.; Li, X.; Sun, J. N-Heterocyclic Carbene Catalyzed *γ*-Dihalomethylenation of Enals by Single-Electron Transfer. *Angew. Chem., Int. Ed.* **2016**, *55*, 15783−15786. (h) Wu, X.; Zhang, Y.; Wang, Y.; Ke, J.; Jeret, M.; Reddi, R. N.; Yang, S.; Song, B.-A.; Chi, Y. R. Polyhalides as Efficient and Mild Oxidants for Oxidative Carbene Organocatalysis by Radical Processes. *Angew. Chem., Int. Ed.* **2017**, *56*, 2942−2946.

(15) (a) Ishii, T.; Kakeno, Y.; Nagao, K.; Ohmiya, H. *N*-Heterocyclic Carbene-Catalyzed Decarboxylative Alkylation of Aldehydes. *J. Am. Chem. Soc.* **2019**, *141*, 3854−3858. (b) Ishii, T.; Ota, K.; Nagao, K.; Ohmiya, H. *N*-Heterocyclic Carbene-Catalyzed Radical Relay Enabling Vicinal Alkylacylation of Alkenes. *J. Am. Chem. Soc.* **2019**, *141*, 14073−14077. (c) Kakeno, Y.; Kusakabe, M.; Nagao, K.; Ohmiya, H. Direct Synthesis of Dialkyl Ketones from Aliphatic Aldehydes through Radical *N*-Heterocyclic Carbene Catalysis. *ACS Catal.* **2020**, *10*, 8524−8529. (d) Matsuki, Y.; Ohnishi, N.; Kakeno, Y.; Takemoto, S.; Ishii, T.; Nagao, K.; Ohmiya, H. Aryl Radical-Mediated N-Heterocyclic Carbene Catalysis. *Nat. Commun.* **2021**, *12*, 3848.

(16) For selected examples on radical NHC catalysis, see (a) Li, J.-L.; Liu, Y.-Q.; Zou, W.-L.; Zeng, R.; Zhang, X.; Liu, Y.; Han, B.; He, Y.; Leng, H.-J.; Li, Q.-Z. Radical Acylfluoroalkylation of Olefins through N-Heterocyclic Carbene Organocatalysis. *Angew. Chem., Int. Ed.* **2020**, *59*, 1863−1870. (b) Kim, I.; Im, H.; Lee, H.; Hong, S. N-Heterocyclic Carbene-Catalyzed Deaminative Cross-Coupling of Aldehydes with Katritzky Pyridinium Salts. *Chem. Sci.* **2020**, *11*, 3192−3197. (c) Gao, Y.; Quan, Y.; Li, Z.; Gao, L.; Zhang, Z.; Zou, X.; Yan, R.; Qu, Y.; Guo, K. Organocatalytic Three-Component 1,2-Cyanoalkylacylation of Alkenes via Radical Relay. *Org. Lett.* **2021**, *23*, 183−189. (d) Yang, H.-B.; Wan, D.-H. C−C Bond Acylation of Oxime Ethers via NHC Catalysis. *Org. Lett.* **2021**, *23*, 1049−1053. (e) Li, Z.; Huang, M.; Zhang, X.; Chen, J.; Huang, Y. N-Heterocyclic Carbene-Catalyzed Four-Component Reaction: Chemoselective $C_{radical}$−$C_{radical}$ Relay Coupling Involving the Homoenolate Intermediate. *ACS Catal.* **2021**, *11*, 10123−10130. (f) Li, Q.-Z.; Zeng, R.; Fan, Y.; Liu, Y.-Q.; Qi, T.; Zhang, X.; Li, J.-L. Remote $C(sp^3)$−H Acylation of Amides and Cascade Cyclization via N-Heterocyclic Carbene Organocatalysis. *Angew. Chem., Int. Ed.* **2022**, *61*, No. e202116629.

(17) For selected reviews on dual NHC/photocatalysis, see: (a) Liu, Q.; Chen, X.-Y. Dual N-Heterocyclic Carbene/Photocatalysis: A New Strategy for Radical Processes. *Org. Chem. Front.* **2020**, *7*, 2082−2087. (b) Mavroskoufis, A.; Jakob, M.; Hopkinson, M. N. Light-Promoted Organocatalysis with N-Heterocyclic Carbenes. *ChemPhotoChem* **2020**, *4*, 5147−5153. (c) Liu, J.; Xing, X.-N.; Huang, J.-H.; Lu, L.-Q.; Xiao, W.-J. Light Opens.; a New Window for N-Heterocyclic Carbene Catalysis. *Chem. Sci.* **2020**, *11*, 10605−10613.

(18) For selected examples on dual NHC/photocatalysis, see: (a) Mavroskoufis, A.; Rajes, K.; Golz, P.; Agrawal, A.; Ruß, V.; Götze, J. P.; Hopkinson, M. N. N-Heterocyclic Carbene Catalyzed Photoenolization/Diels−Alder Reaction of Acid Fluorides. *Angew. Chem., Int. Ed.* **2020**, *59*, 3190−3194. (b) Bay, A. V.; Fitzpatrick, K. P.; Betori, R. C.; Scheidt, K. A. Combined Photoredox and Carbene Catalysis for the Synthesis of Ketones from Carboxylic Acids. *Angew. Chem., Int. Ed.* **2020**, *59*, 9143−9148. (c) Meng, Q.-Y.; Döben, N.; Studer, A. Cooperative NHC and Photoredox Catalysis for the Synthesis of *β*-Trifluoromethylated Alkyl Aryl Ketones. *Angew. Chem., Int. Ed.* **2020**, *59*, 19956−19960. (d) Liu, M.-S.; Shu, W. Catalytic, Metal-Free Amide Synthesis from Aldehydes and Imines Enabled by a Dual-Catalyzed Umpolung Strategy under Redox-Neutral Conditions. *ACS Catal.* **2020**, *10*, 12960−12966. (e) Liu, K.; Studer, A. Direct *α*-Acylation of Alkenes via N-Heterocyclic Carbene, Sulfinate, and Photoredox Cooperative Triple Catalysis. *J. Am. Chem. Soc.* **2021**, *143*, 4903−4909. (f) Meng, Q.-Y.; Lezius, L.; Studer, A. Benzylic C−H Acylation by Cooperative NHC and Photoredox Catalysis. *Nat. Commun.* **2021**, *12*, 2068. (g) Sato, Y.; Goto, Y.; Nakamura, K.; Miyamoto, Y.; Sumida, Y.; Ohmiya, H. Light-Driven N-Heterocyclic Carbene Catalysis Using Alkylborates. *ACS Catal.* **2021**, *11*, 12886−12892. (h) Bay, A. V.; Fitzpatrick, K. P.; González-Montiel, G. A.; Farah, A. O.; Cheong, P. H.-Y.; Scheidt, K. A. Light-Driven Carbene Catalysis for the Synthesis of Aliphatic and *α*-Amino Ketones. *Angew. Chem., Int. Ed.* **2021**, *60*, 17925−17931. (i) Zuo, Z.; Daniliuc, C. G.; Studer, A. Cooperative NHC/Photoredox Catalyzed Ring-Opening of Aryl Cyclopropanes to 1-Aroyloxylated-3-Acylated Alkanes. *Angew. Chem., Int. Ed.* **2021**, *60*, 25252−25257. (j) Yu, X.; Meng, Q.-Y.; Daniliuc, C. G.; Studer, A. Aroyl Fluorides as Bifunctional Reagents for Dearomatizing Fluoroaroylation of Benzofurans. *J. Am. Chem. Soc.* **2022**, *144*, 7072−7079.

(19) For recent examples, see: (a) Miller, D. C.; Choi, G. J.; Orbe, H. S.; Knowles, R. R. Catalytic Olefin Hydroamidation Enabled by Proton-Coupled Electron Transfer. *J. Am. Chem. Soc.* **2015**, *137*, 13492−13495. (b) Davies, J.; Svejstrup, T. D.; Fernandez Reina, D.; Sheikh, N. S.; Leonori, D. Visible-Light-Mediated Synthesis of Amidyl Radicals: Transition Metal-Free Hydroamination and *N*-Arylation Reactions. *J. Am. Chem. Soc.* **2016**, *138*, 8092−8095. (c) Ren, X.; Guo, Q.; Chen, J.; Xie, H.; Xu, Q.; Lu, Z. Visible-Light Promoted Diastereodivergent Intramolecular Oxyamidation of Alkenes. *Chem. − Eur. J.* **2016**, *22*, 18695−18699. (d) Fernandez Reina, D.; Dauncey, E. M.; Morcillo, S. P.; Svejstrup, T. D.; Popescu, M. V.; Douglas, J. J.; Sheikh, N. S.; Leonori, D. Visible-Light-Mediated 5-exo-dig Cyclizations of Amidyl Radicals. *Eur. J. Org. Chem.* **2017**, *2017*, 2108−2111. (e) Nguyen, S. T.; Zhu, Q.; Knowles, R. R. PCET-Enabled Olefin Hydroamidation Reactions with *N*-Alkyl Amides. *ACS Catal.* **2019**, *9*, 4502−4507. (f) Zheng, S.; Zhang, S.-Q.; Saeednia, B.; Zhou, J.; Anna, J. M.; Hong, X.; Molander, G. A. Diastereoselective Olefin Amidoacylation via Photoredox PCET/Nickel-Dual Catalysis: Reaction Scope and Mechanistic Insights. *Chem. Sci.* **2020**, *11*, 4131−4137.

(20) See the Supporting Information for detail.

(21) Michael, J. P. Indolizidine and Quinolizidine Alkaloids. *Nat. Prod. Rep.* **2008**, *25*, 139−165.

(22) Ren, S.-C.; Lv, W.-X.; Yang, X.; Yan, J.-L.; Xu, J.; Wang, F.-X.; Hao, L.; Chai, H.; Jin, Z.; Chi, Y. R. Carbene-Catalyzed Alkylation of Carboxylic Esters via Direct Photoexcitation of Acyl Azolium Intermediates. *ACS Catal.* **2021**, *11*, 2925−2934.

(23) For a ground-state electron transfer between **A1** and **1a**, the Gibbs free energy (ΔG_{SET}) is expressed by the equation: $\Delta G_{SET} = E^{ox}[\mathbf{B1}/\mathbf{A1}] - E^{red}[\mathbf{1a}/\mathbf{1a}^{\cdot-}] + \Delta E_{coulombic}$.

(24) (a) Farid, S.; Dinnocenzo, J. P.; Merkel, P. B.; Young, R. H.; Shukla, D.; Guirado, G. Reexamination of the Rehm−Weller Data Set Reveals Electron Transfer Quenching That Follows a Sandros−Boltzmann Dependence on Free Energy. *J. Am. Chem. Soc.* **2011**, *133*, 11580−11587. (b) Buzzetti, L.; Crisenza, G. E. M.; Melchiorre, P. Mechanistic Studies in Photocatalysis. *Angew. Chem., Int. Ed.* **2019**, *58*, 3730−3747.

(25) For the iminoacylation with chiral NHC, see the Supporting Information for details.

(26) For a radical trapping experiment with TEMPO, see the Supporting Information.

(27) (a) Sutcliffe, R.; Griller, D.; Lessard, J.; Ingold, K. U. The Structure of Amidyl Radicals. Evidence for the π-Electronic Ground State and for Twist about the Acyl-Nitrogen Bond by Electron Paramagnetic Resonance Spectroscopy. *J. Am. Chem. Soc.* **1981**, *103*, 624−628. (b) Esker, J. L.; Newcomb, M. Chemistry of Amidyl Radicals Produced from N-Hydroxypyridine-2-thione Imidate Esters. *J. Org. Chem.* **1993**, *58*, 4933−4940. (c) Horner, J. H.; Musa, O. M.; Bouvier, A.; Newcomb, M. Absolute Kinetics of Amidyl Radical Reactions. *J. Am. Chem. Soc.* **1998**, *120*, 7738−7748.

(28) For the X-ray structure of **91**, see the Supporting Information for detail.

https://doi.org/10.1021/jacs.2c11209
J. Am. Chem. Soc. 2022, 144, 22767−22777